

Tryptophan Synthase: Structure and Function of the Monovalent Cation Site[†]

Adam T. Dierkers,^{‡,||} Dimitri Niks,[‡] Ilme Schlichting,[§] and Michael F. Dunn*,[‡]

[‡]Department of Biochemistry, University of California, Riverside, California 92521, and [§]Department of Biomolecular Mechanisms, Max Planck Institute for Medical Research, Heidelberg, Germany ^{||}Present address: School of Molecular and Microbial Biosciences, University of Sydney, Sydney, Australia.

Received May 17, 2009; Revised Manuscript Received October 22, 2009

ABSTRACT: The monovalent cation (MVC) site of the tryptophan synthase from *Salmonella typhimurium* plays essential roles in catalysis and in the regulation of substrate channeling. In vitro, MVCs affect the equilibrium distribution of intermediates formed in the reaction of L-Ser with the $\alpha_2\beta_2$ complex; the MVC-free, Cs⁺-bound, and NH₄⁺-bound enzymes stabilize the α -aminoacrylate species, E(A-A), while Na⁺ binding stabilizes the L-Ser external aldimine species, E(Aex₁). Two probes of β -site reactivity and conformation were used herein, the reactive indole analogue, indoline, and the L-Trp analogue, L-His. MVC-bound E(A-A) reacts rapidly with indoline to give the indoline quinonoid species, E(Q)_{indoline}, which slowly converts to dihydroiso-L-tryptophan. MVC-free E(A-A) gives very little E(Q)_{indoline}, and turnover is strongly impaired; the fraction of E(Q)_{indoline} formed is <3.5% of that given by the Na⁺-bound form. The reaction of L-Ser with the MVC-free internal aldimine species, E(Ain), initially gives small amounts of an active E(A-A) which converts to an inactive species on a slower, conformational, time scale. This inactivation is abolished by the binding of MVCs. The inactive E(A-A) appears to have a closed β -subunit conformation with an altered substrate binding site that is different from the known conformations of tryptophan synthase. Reaction of L-His with E(Ain) gives an equilibrating mixture of external aldimine and quinonoid species, E(Aex)_{his} and E(Q)_{his}. The MVC-free and Na⁺ forms of the enzyme gave trace amounts of E(Q)_{his} (~1% of the β -sites). The Cs⁺ and NH₄⁺ forms gave ~17 and ~14%, respectively. The reactivity of MVC-free E(Ain) was restored by the binding of an α -site ligand. These studies show MVCs and α -site ligands act synergistically to modulate the switching of the β -subunit from the open to the closed conformation, and this switching is crucial to the regulation of β -site catalytic activity. Comparison of the structures of Na⁺ and Cs⁺ forms of the enzyme shows Cs⁺ favors complexes with open indole binding sites poised for the conformational transition to the closed state, whereas the Na⁺ form does not. The β -subunits of Cs⁺ complexes exhibit preformed indole subsites; the indole subsites of the open Na⁺ complexes are collapsed, distorted, and too small to accommodate indole.

The tryptophan synthase from *Salmonella typhimurium* is a substrate-channeling bienzyme complex that catalyzes the last two steps in the biosynthesis of L-Trp (Scheme 1) (1–5). The

*Supported by National Institutes of Health Grant GM5574 (M.F.D.) and Deutsche Forschungsgemeinschaft (I.S.).

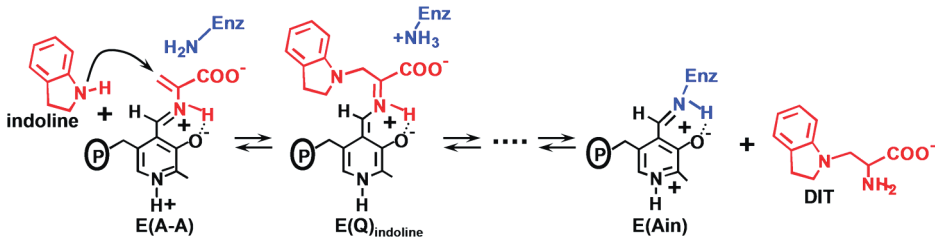
[†]To whom correspondence should be addressed. Telephone: (951) 827-4235. Fax: (951) 827-4434. E-mail: Michael.dunn@ucr.edu.

[‡]Abbreviations: $\alpha_2\beta_2$, native form of tryptophan synthase from *S. typhimurium*; α , α -subunit; β , β -subunit; E(Ain), internal aldimine (Schiff base) species; E(Aex₁), external aldimine species formed between the PLP cofactor and L-Ser; E(GD), gem-diamine species; E(A-A), α -aminoacrylate Schiff base species; E(Q₁), L-Ser quinonoid species; E(Q₃) and E(Q)_{indoline}, quinonoid species that accumulate in the reaction between E(A-A) and indole and between E(A-A) and indoline, respectively; E(Aex₂), L-Trp external aldimine species; PLP, pyridoxal phosphate; L-Ser, L-serine; L-Trp, L-tryptophan; IGP, 3-indole-D-glycerol 3'-phosphate; GP, α -D,L-glycerol phosphate; G3P, D-glyceraldehyde 3-phosphate; DIT, dihydroiso-L-tryptophan; ASL, α -site ligand; F9, N-(4'-trifluoromethoxybenzenesulfonyl)-2-aminoethyl phosphate; ANS, 8-anilino-1-naphthalene sulfonate; β -me, β -mercaptoethanol; DTNB, dithiobis(2-nitrobenzoic acid); TNB, 2-nitro-5-thiobenzoic acid; TEA, triethanolamine; MVC, monovalent cation; K_{Dapp} , apparent dissociation constant; SWSF, single-wavelength stopped-flow; RSSF, rapid-scanning stopped-flow; PDB, Protein Data Bank. Structural elements of tryptophan synthase are designated as follows: loop α L2, α 53– α 60; loop α L6, α 179– α 193; helix α H8, α 249– α 265; COMM domain, β 102– β 189; helix β H5, β 145– β 150; helix β H6, β 165– β 181.

β -active site of this enzyme complex is activated by a monovalent cation (MVC)¹ binding to an allosteric site (6–10) located near the PLP cofactor (viz., the Cs⁺ site shown in Figure 1). In vitro, the enzyme can bind Na⁺, K⁺, Cs⁺, Li⁺, Rb⁺, NH₄⁺, or guanidinium ion (6–11) at this site. These MVC complexes and the MVC-free form each exert different structural effects on the enzyme that alter the kinetic and thermodynamic properties of the β -subunit catalytic cycle, and the allosteric interactions linking the α - and β -sites (5, 7–10).

The α - and β -reactions catalyzed by tryptophan synthase are depicted in Scheme 1. The top panel shows the α -subunit-catalyzed conversion of 3-indole-D-glycerol 3'-phosphate (IGP) to indole and D-glyceraldehyde 3-phosphate (G3P) via an intermediate in which the indole ring of IGP is protonated at C-3 (3, 5). The β -reaction (Scheme 1, bottom panel) occurs in two stages. In stage I, L-Ser reacts with the internal aldimine form of the enzyme, E(Ain), to give the external aldimine species, E(Aex₁), the L-Ser quinonoid species, E(Q₁), and then the α -aminoacrylate species, E(A-A). As stage I approaches equilibrium, two intermediates dominate, E(Aex₁) ($\lambda_{max} = 424$ nm) and E(A-A) ($\lambda_{max} = 350$ and 460 nm) (12–16). The ratio of E(Aex₁) to E(A-A) is sensitive to the type of MVC bound; e.g., Na⁺ favors E(Aex₁), while Cs⁺ favors E(A-A) (9, 11).

The α -reaction is switched on by the conversion of E(Aex₁) to E(A-A) at the β -site during stage I of the β -reaction. The α -reaction is switched off when E(Q₃) is converted to E(Aex₂) in stage II (5). To initiate stage II of the β -reaction, indole formed in the α -reaction is transferred (channeled) from the α -catalytic site to the β -catalytic site via the ~25 Å long interconnecting tunnel (dashed white line in Figure 1A) where it reacts with E(A-A). MVC-bound forms of E(A-A) react quickly with indole and indole analogues such as indoline, to form quinonoid species that then undergo further transformation to give the corresponding



The X-ray structure of the E(Q)_{indoline} complex presented in Figure 1A,B shows the closed conformation of the $\alpha\beta$ -dimeric unit of the $\alpha_2\beta_2$ tetrameric complex (5, 20). At the closed β -site (Figure 1B), the indoline moiety, in the form of the indoline quinonoid species, E(Q)_{indoline}, is bound to the indole ring subsite and is poised for conversion to the corresponding external aldimine (20). Figure 1B also shows the β -site catalytic groups β Lys87 and β Glu109, along with the salt bridge formed between β Arg141 and β Asp305 and H-bonds involving β Ser297 and β Ser299, interactions that are crucially important for stabilization of the closed conformation (5, 20, 22).

Figure 1A shows a transition-state analogue bound to the α -site. This analogue consists of an adduct formed between indoline and G3P. The acid–base catalytic residue, α Glu49, is H-bonded to this adduct (5, 20). The residue that plays a charge stabilization role in catalysis, α Asp60, is also shown (5, 20).

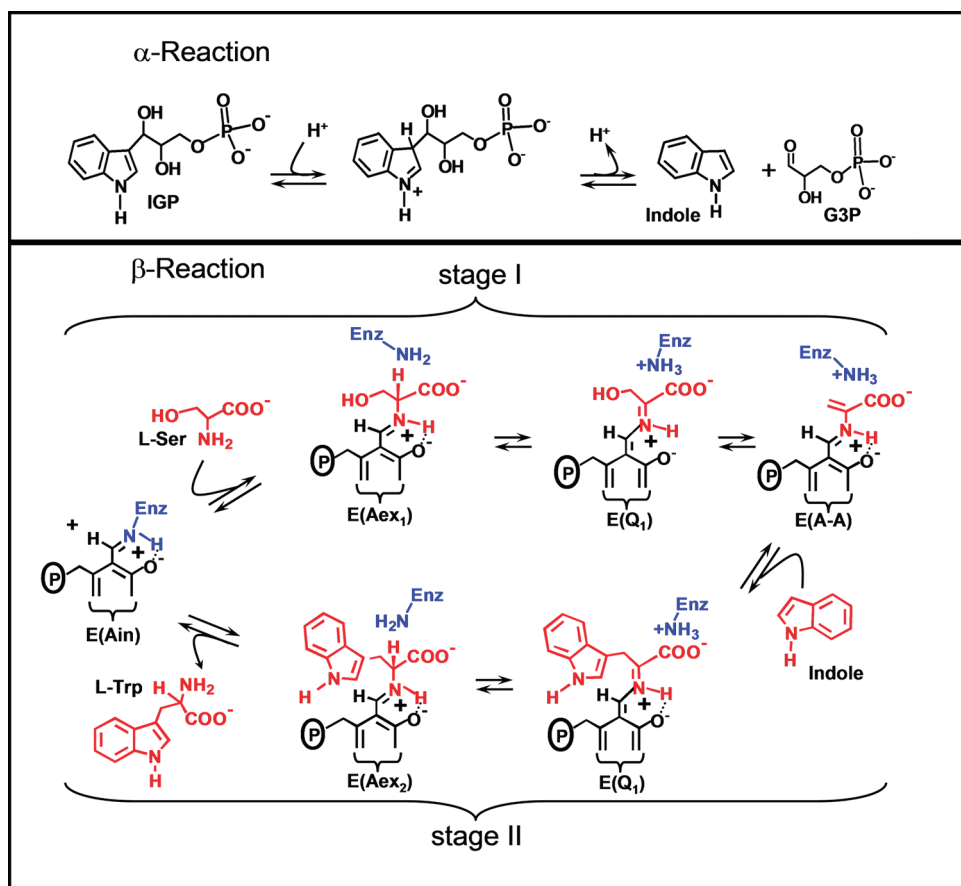
The activities of many enzymes, including tryptophan synthase, are known to be modulated by MVC effectors (6–11, 23–26). MVC activation and deactivation of enzyme catalysis have evolved to modulate biological function in a surprisingly large number of enzymes. In recent years, X-ray structure studies have provided detailed information about the nature of MVC binding sites; however, there is still relatively little known about the detailed mechanisms by which MVC binding brings about activation and deactivation of catalytic activity and biological function. Like conservative site-directed mutations, MVC substitution provides a means for creating subtle structural perturbations in MVC-activated enzymes that have the potential for revealing important structure–function relationships (25). The expected structural changes due to substitution of one MVC for another are relatively small due to the small change in the ionic radius (for example, replacement of Na⁺ with Cs⁺ increases the ionic radius by ~0.77 Å). Therefore, MVC substitutions often produce subtle structural changes with significant kinetic effects (25). In the tryptophan synthase system, as measured by the ratio k_{cat}/K_m , Peracchi et al. reported an ~45-fold activation due to the binding of Na⁺ to the MVC-free enzyme (7). Woehl et al. (8) discovered that the binding of a monovalent cation to tryptophan synthase is essential both to β -site catalysis and to intersubunit

new amino acids (Scheme 1, stage II) (2–5, 12, 13, 17–20). The binding of α -site ligands activates the rate-limiting step in stage I of the β -reaction, the conversion of E(Aex₁) to E(A-A) (4, 5, 21, 22). The switching between low and high states of catalytic activity is coupled to the switching of $\alpha\beta$ -dimeric units of the enzyme complex between open and closed conformations (5, 18, 19, 22).

The indole analogue, indoline, reacts rapidly and reversibly with E(A-A) to give the indoline quinonoid species, E(Q)_{indoline}, a quasi-stable intermediate with an intense absorption band at 466 nm ($\epsilon > 40000 \text{ M}^{-1} \text{ cm}^{-1}$) (17–20) (eq 1).

communication. They found that in comparison to the Na⁺ form of the enzyme, the activity of the MVC-free form is greatly altered in both stages I and II of the β -reaction (Scheme 1). The MVC-free enzyme exhibits a turnover rate for the β -reaction that is decreased 5- and 6.4-fold relative to those of the Na⁺- and K⁺-substituted enzymes, respectively (8), and the $\alpha\beta$ -reaction is similarly affected (27). The most interesting effects involve the allosteric communication between the α - and β -sites. Reactions of L-Ser at the β -site with the Na⁺, K⁺, and NH₄⁺ forms of the enzyme activate the α -site by ~30-, 26-, and 40-fold, respectively (27). When all monovalent metal ions are removed, reaction of L-Ser at the β -site does not activate the α -reaction (7–10, 27). Rhee et al. (6) showed that the MVC site is located in the β -subunit near the β -catalytic site (see Figure 1). The fraction of β -sites in the form of E(Q)_{indoline} is dependent on the particular MVC bound, while the MVC-free species gives almost no E(Q)_{indoline}. The amount of E(Q)_{indoline} formed in the MVC-free system is less than 10% of that formed with the Na⁺-substituted enzyme (27). Kinetic, spectroscopic, and X-ray structural studies (4, 5, 8–10, 15, 16, 18–22) have shown that E(Ain) and E(Aex) species favor the open conformation of the β -subunit, while the E(Q) and E(A-A) species favor the closed conformation. Previous investigators (5, 8–10, 22) have proposed that the chemistry catalyzed by the β -site preferentially occurs via intermediates with the closed conformation, and that the switch from the open to the closed conformation is mediated by ligand binding to the α -subunit, by MVC binding to the β -subunit, and by the conversion of E(Aex₁) to E(Q) and E(A-A).

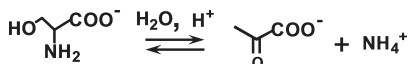
Figure 1B shows the relationship of the MVC site to the β -catalytic site. The MVC site cavity is formed by the carbonyl oxygens of six amino acid residues, β Val231, β Gly232, β Gly268, β Leu304, β Phe306, and β Ser308. Cs⁺ fills this cavity and forms coordination bonds with all six of these carbonyl oxygens (Figure 1B). Because of the smaller ionic radius of Na⁺, this ion bonds to only three of the six carbonyls (β Gly232, β Phe306, and β Ser308), and two waters are incorporated into the coordination sphere (4–6, 20–22). The coordination of K⁺ is similar to that of Na⁺ except that only a single water is included in the coordination sphere (6). Inspection of Figure 1B shows that the MVC site is linked to two residues with important roles in β -site

Scheme 1: Organic Chemistry of the α - and β -Reactions

function, β Phe306 and β Asp305 (5, 22). The aromatic ring of β Phe306 forms part of the binding site for the substrate, indole. β Asp305, situated between MVC ligands β Leu304 and β Phe306, plays an important role in the switching between open and closed conformational states. In the open, inactive conformation, the β Asp305 carboxylate is H-bonded to the Aex₁ hydroxyl. This interaction stabilizes E(Aex₁) by holding the Aex₁ hydroxyl away from the acid–base catalytic group, β Glu109. The switch to the closed conformation ruptures this H-bond and repositions the carboxylate of β Asp305 to form the salt bridge with β Arg141, allowing the Aex₁ hydroxyl to rotate into position for the β Glu109-catalyzed elimination (5, 22). Consequently, the MVC site is directly involved in indole binding, the conformational switch, and β -site catalysis.

This work undertakes detailed studies of the MVC-free, Na^+ -bound, and Cs^+ -bound forms of tryptophan synthase in further investigating the effects of MVC binding on the catalytic activity and conformational states of the enzyme. The 466 nm spectroscopic signature of $E(Q)_{indoline}$ is used to quantify the reactivities of the MVC-free and MVC-bound E(A-A) species (27). The L-Trp analogue, L-His, is used to investigate stage II of the β -reaction. L-His reacts at the β -site to give a distribution of intermediates dominated by the L-His external aldimine, E(Aex)_{his}, and the L-His quinonoid species, E(Q)_{his}. It will be shown that the distribution of these two species is modulated by MVC binding to the β -site and by ligand binding to the α -site. We also examine the effects of α -site ligand binding on the switching between open and closed conformational states using the IGP analogue, *N*-(4'-trifluoromethoxybenzenesulfonyl)-2-aminoethyl phosphate (F9) (21, 22). F9 is chemically

stable, binds tightly to the α -site, and mimics the allosteric effects of IGP and G3P (22). The results presented herein reveal the following. (i) Despite the observable formation of a closed conformation, MVC-free E(A-A) is unreactive toward indoline. (ii) The slow turnover of L-Ser to pyruvate and NH_4^+ when L-Ser is incubated with the MVC-free enzyme (the pyruvate side reaction, eq 2)



generates traces of NH_4^+ that activate the enzyme by binding to the MVC site. This activation obscures the near-zero reactivity of MVC-free E(A-A) in the reaction with indoline. (iii) Reaction of L-Ser with E(Ain) initially gives two forms of E(A-A), one reactive and the other inactive; the reactive form converts to the inactive form on a slower time scale. (iv) The binding of MVCs influences the distribution of the two forms of E(A-A), strongly favoring the reactive form. The likely conformational origins of inactive MVC-free E(A-A) are discussed within the context of known β -site structures and the switching between active and inactive conformational states. (v) The Cs^+ forms of the open β -subunit conformation are set up for conversion to the closed state with preformed indole binding subsites; the corresponding Na^+ forms are not set up for conversion to the closed state, and the indole subsites are distorted with dimensions too small to accommodate indole. (vi) MVC-bound forms of the enzyme balance the relative energies of the open and closed conformations of the β -subunit during catalysis, thereby modulating the switching

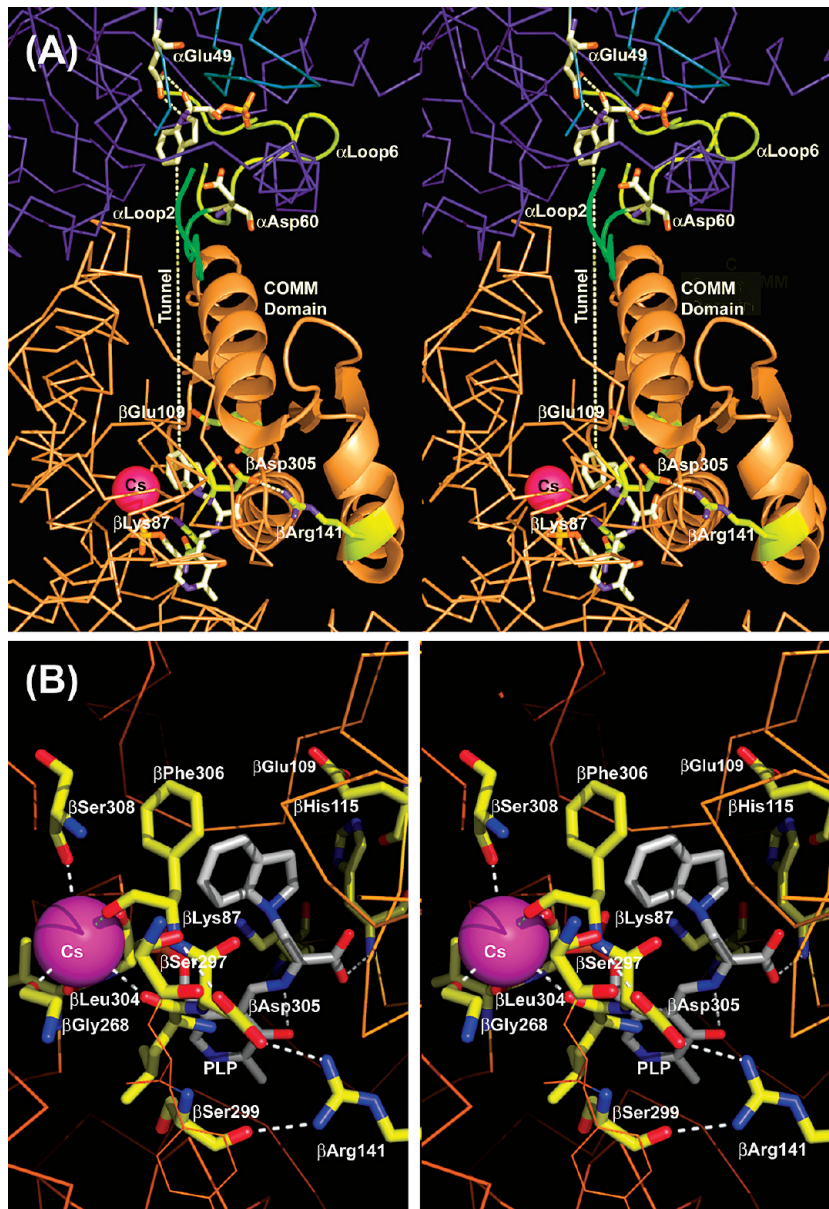


FIGURE 1: Stereoview of the structure of an $\alpha\beta$ -dimeric unit of $E(Q)$ indoline and details of the β -catalytic site. (A) Stereoview of the catalytic sites of the α - and β -subunits, the MVC site, and interconnecting tunnel. The dashed white line indicates the approximate position of the tunnel. The transition-state analogue formed by the reaction of indoline with G3P at the α -site and the quinonoid intermediate at the β -site are shown as sticks. Cs^+ is shown as a magenta sphere. The α -subunit is represented by a backbone structure colored blue, and the β -subunit is colored tan. Loop $\alpha L2$ and loop $\alpha L6$ are shown as green and yellow ribbons, respectively. The COMM domain is shown as a cartoon ribbon and the remainder of the β -subunit as a backbone. At the α -site, catalytic residues α Glu49 and α Asp60 and the adduct formed between indoline and G3P are shown in CPK-colored sticks. At the β -site, catalytic residues β Lys87 and β Glu109 and the salt bridging residues β Arg141 and β Asp305 are shown as sticks with C atoms colored yellow, N atoms blue, and O atoms red. The structure of the indoline quinonoid intermediate is shown as CPK-colored sticks. (B) Stereoview of the β -catalytic site with the PLP-bound indoline quinonoid intermediate shown as CPK-colored sticks. Catalytic residues β Lys87 and β Glu109, the β Asp305– β Arg141 salt bridge, H-bonding residues β Ser299 and β Ser297, indole subsite residues β His115 and β Phe306, and Cs^+ ligands β Gly268, β Leu304, β Phe306, and β Ser308 are shown as sticks with C atoms colored yellow, N atoms blue, and O atoms red. Cs^+ is shown as a purple sphere. H-Bonding interactions and coordination bonds to Cs^+ are shown as white dashed lines. The β -subunit is represented as an orange backbone. Structures are drawn from PDB entry 3CEP with PyMOL version 1.1r1.

between open and closed states which synchronizes the α - and β -catalytic cycles.

MATERIALS AND METHODS

Materials. L-Ser, L-His, indoline, CsCl, NaCl, and NH₄Cl were purchased from Sigma-Aldrich. Indoline was purified as previously described (17). N-(4-Trifluoromethoxybenzenesulfonyl)-2-amino-1-ethyl phosphate (F9) was synthesized as described previously (22). 5,5'-Dithiobis(2-nitrobenzoic acid) (DTNB)

was purchased from Calbiochem. All solutions were prepared at $25 \pm 2^\circ\text{C}$ and maintained at pH 7.8 in 50 mM triethanolamine (TEA) buffer and (except for H⁺) maintained MVC-free. F9 was prepared free of monovalent metal ions by exchange of Na⁺ with cyclohexylammonium chloride. *S. typhimurium* $\alpha_2\beta_2$ tryptophan synthase was purified as previously described (28).

UV–Visible Static and Stopped-Flow Spectral Measurements. Static UV–vis absorbance spectra were recorded on a Hewlett-Packard 8452A diode array spectrophotometer at

25 ± 2 °C in 50 mM TEA buffer (pH 7.8). Titration curves were fitted to eq 3 using Sigma Plot 9.0

$$A = \frac{[\text{titrant}](A_t - A_0)}{K_{\text{dapp}} + [\text{titrant}]} \quad (3)$$

where A is the observed absorbance, A_0 is the absorbance at time zero, and A_{fin} is absorbance extrapolated to infinite titrant concentration.

Measurement of the rate of pyruvate formation was accomplished through monitoring the absorption maximum for pyruvate at 316 nm ($\epsilon_{316} = 22.7 \text{ M}^{-1} \text{ cm}^{-1}$). The turnover rate for conversion of L-Ser and β -me to S-hydroxyethyl-L-cysteine was assayed by trapping unreacted β -me with DTNB and measuring production of 2-nitro-5-thiobenzoic acid (TNB), at 410 nm ($\epsilon_{410} = 14150 \text{ M}^{-1} \text{ cm}^{-1}$) (29). Single-wavelength and rapid-scanning stopped-flow measurements were preformed as previously described (9, 10). Single-wavelength time courses were fitted using the Levenberg–Marquardt algorithm shown in eq 4

$$A = A_0 \pm \sum A_n e \left(\frac{-t}{\tau} \right) \quad (4)$$

where A and A_0 are absorbance values at time t and time infinity, respectively, and A_n is the amplitude of the n th relaxation, τ_n .

Kinetic Simulations. Kinetic simulations were preformed using Kinetic version 3.11 (30) and are described in the Supporting Information.

Structure Alignments. Structures were overlaid several different ways. It was found that overlaying the Co atoms of residues 10–100 of the β -subunit using PyMOL version 1.1r1 gave alignments very similar to those reported by Rhee et al. (6) for comparison of the E(Ain) structures (PDB entries 1BKS and 1TTP) and the E(Q)_{indoline} structure (PDB entry 3CEP). This region of the β -subunit appears particularly insensitive to the conformational differences between open and closed states. Thus, all of the subunit alignments discussed in this work were performed using this selection of atoms. Alignments to compare β -active sites of different MVC complexes and different conformation states were accomplished with PyMOL using paired selections consisting of atoms in the PLP cofactor and the MVC.

RESULTS

Reactions of L-Ser, and L-Ser and Indoline, with MVC-Bound and -Free Forms of $\alpha_2\beta_2$. The UV-vis spectroscopic properties of the PLP intermediates bound to tryptophan synthase provide sensitive probes of the conformational states of tryptophan synthase. Solution studies and X-ray structures have shown that the MVC-bound internal and external aldimine intermediates have the open conformation, while the α -aminoacrylate and quinonoid intermediates have the closed conformation (3, 5, 15, 16, 18–22). The reaction of L-Ser with the MVC-bound and -free forms of $\alpha_2\beta_2$ results in the formation of equilibrating mixtures dominated by E(Aex₁) ($\lambda_{\text{max}} = 424 \text{ nm}$) and E(A-A) ($\lambda_{\text{max}} = 350$ and 460 nm) (9–11, 13, 14, 31–33). Figure 2A compares the static spectra for the reaction of L-Ser in the presence or absence of Na⁺, Cs⁺, or NH₄⁺. These spectra show that in the Cs⁺, NH₄⁺, or MVC-free forms, the equilibrium distribution favors E(A-A), while the Na⁺ form favors E(Aex₁). The relaxation rates for formation of E(Aex₁) with the Na⁺, K⁺, NH₄⁺, and Cs⁺ forms are 900, 660, 420, and 250 s⁻¹, respectively, whereas the rates for conversion of E(Aex₁) to E(A-A) are 7, 20, 90, and 70 s⁻¹, respectively. The MVC-free form gives rates of

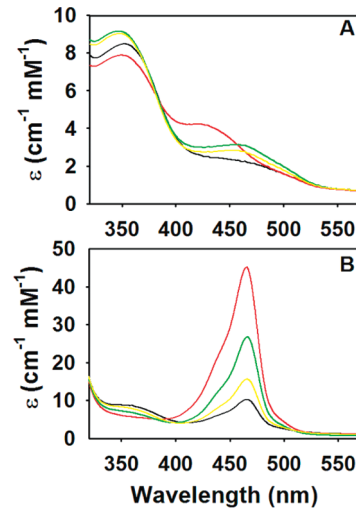


FIGURE 2: Comparison of MVC-induced effects on the static UV-vis spectra of tryptophan synthase: (A) L-Ser reaction and (B) indoline reaction. (A) Reaction of MVC-bound and free $\alpha_2\beta_2$ with L-Ser (stage I, β -reaction). (B) Reaction of $\alpha_2\beta_2$ with L-Ser and indoline (the indoline reaction). Color code: red for the Na⁺ form, yellow for the NH₄⁺ form, green for the Cs⁺ form, and black for the MVC-free form. Final concentrations: 20 μM $\alpha_2\beta_2$, 50 mM L-Ser, 5 mM indoline, and 50 mM MVC.

200 and 21 s⁻¹ for formation and decay of E(Aex₁), respectively (27, 34).

Spectra for the reaction of E(A-A) with indoline (the indoline reaction) are presented in Figure 2B. The MVC-bound forms of E(A-A) react with indoline to generate E(Q)_{indoline} ($\lambda_{\text{max}} = 466 \text{ nm}$; $\epsilon_{\text{max}} > 60000 \text{ M}^{-1} \text{ cm}^{-1}$); however, as indicated by the small amount of E(Q)_{indoline} generated, the MVC-free form is severely impaired (8–10). Figure 2B shows that Na⁺ is more effective than NH₄⁺ or Cs⁺ in stabilizing E(Q)_{indoline}, and that under similar conditions very little E(Q)_{indoline} is formed with the MVC-free system. The relative order of effectiveness is as follows: Na⁺ > Cs⁺ > NH₄⁺ ≫ MVC-free. The smaller yields obtained with NH₄⁺ and with Cs⁺ reflect larger apparent dissociation constants for indoline in the reaction with E(A-A); the 5.0 mM indoline used in Figure 2B is subsaturating for these MVCs. These spectral data indicate that the affinity of the MVC-free E(A-A) for indoline is at least 50–100-fold weaker than the affinities of the NH₄⁺- or Cs⁺-bound E(A-A) species.

The appearance of the 466 nm spectral band in the indoline reaction (Figure 2B) occurs in two kinetic phases. Most of the amplitude change occurs with a relatively fast relaxation rate ($1/\tau_1 \approx 700 \text{ s}^{-1}$). The amplitude of the slower phase is very small, and therefore, this phase was not considered further in the effort to characterize the reactivity of the MVC-free enzyme.

Pyruvate and NH₄⁺ Formation in the L-Ser Reaction. In previous work, the impaired catalytic properties of the MVC-free enzyme were not sufficiently quantified to determine the extent to which MVC-free E(A-A) is unreactive toward nucleophiles. Because both MVC-bound and MVC-free forms of E(A-A) undergo a slow side reaction with water to give pyruvate and NH₄⁺ with regeneration of E(Ain) (eq 2), experiments in which the enzyme and excess L-Ser are preincubated result in the steady-state production of NH₄⁺, a contaminating MVC. The rate of the pyruvate side reaction depends on the ligation state of the α -site, and the particular MVC bound to the MVC site (34). To test the MVC effect for the conditions employed in these studies, the rate of pyruvate formation from L-Ser catalyzed by MVC-free or

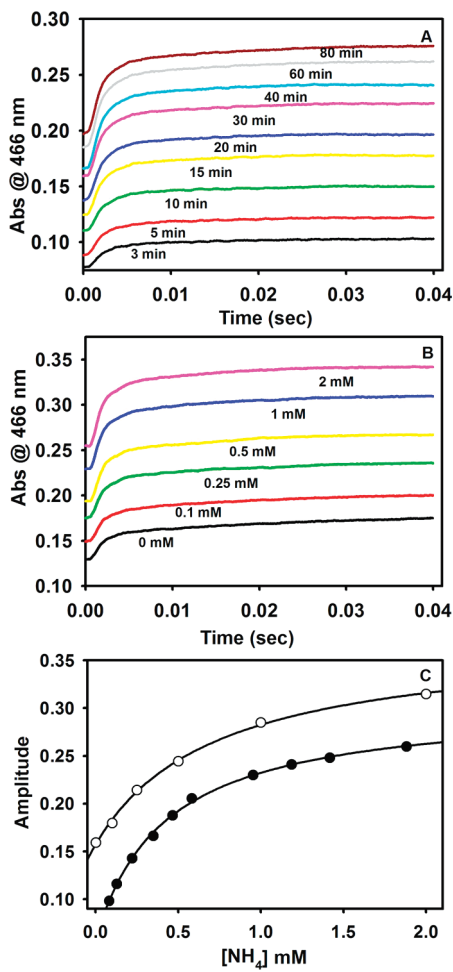


FIGURE 3: Ammonium ion contamination effects from deamination of L-Ser in the tryptophan synthase-catalyzed pyruvate side reaction. (A) Effects of incubation of L-Ser and $\alpha_2\beta_2$ on the indoline reaction (incubation times indicated). Final concentrations were 10 μM $\alpha_2\beta_2$, 50 mM L-Ser, and 5 mM indoline. (B) Effects of NH_4^+ preincubation with $\alpha_2\beta_2$. Final concentrations were 10 μM $\alpha_2\beta_2$, 50 mM L-Ser, 5 mM indoline, and the indicated NH_4^+ concentration. Time courses in panels A and B were measured using SWSF instrumentation. (C) Comparison of the effect of L-Ser incubation time (●) on amplitude with the effects of added $[\text{NH}_4^+]$ (○) on the fast phase of the indoline reaction ($\alpha_2\beta_2$ preincubated with NH_4^+). Amplitudes were taken from panels A and B. To correct for fast phase amplitude loss in the instrument dead time, the total amplitude of the fast phase was estimated as the sum of the observed fast phase and the y-intercept value for the reaction of $\alpha_2\beta_2$ and L-Ser with indoline. Traces were fit to the sum of two exponentials. The NH_4^+ concentrations for time-resolved data points (●) were estimated using a k_{cat} of 0.098 s^{-1} for pyruvate formation at each incubation time in panel A.

NH_4^+ -, Cs^+ -, or Na^+ -bound $\alpha_2\beta_2$ was measured by recording the absorbance change due to the appearance of pyruvate at 316 nm ($\Delta\varepsilon_{316} = 22.7 \text{ M}^{-1} \text{ cm}^{-1}$), at varying L-Ser incubation times. The MVC-free, NH_4^+ , and Cs^+ forms of the enzyme all gave similar turnover rates ($k_{\text{cat}} = 0.008 \pm 0.002 \text{ s}^{-1}$), while the turnover rate for the Na^+ form ($k_{\text{cat}} = 0.09 \pm 0.002 \text{ s}^{-1}$) was ~11-fold greater.

Influence of L-Ser Incubation Time and NH_4^+ Production on the Indoline Reaction. To quantify the effects of NH_4^+ on the activity of the MVC-free enzyme, experiments were performed to determine the significance of NH_4^+ contamination from the pyruvate side reaction on preparations of the MVC-free enzyme. Figure 3A compares the time courses for the indoline reaction obtained under conditions where $\alpha_2\beta_2$ (prepared MVC-free) and L-Ser were preincubated prior to reaction for time

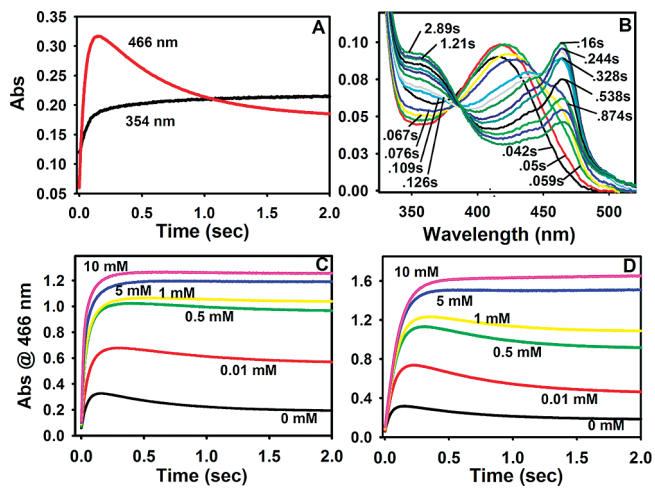


FIGURE 4: (A) Comparison of the indoline reaction time courses at 466 and 354 nm under MVC-free conditions where L-Ser is mixed with 20 μM $\alpha_2\beta_2$ preincubated with indoline in the SWSF apparatus. (B) Rapid-scanning stopped-flow experiment showing time-resolved spectra (from 300 to 550 nm) for the formation of E(Q)_{indoline} under MVC-free conditions. L-Ser was mixed with 10 μM MVC-free $\alpha_2\beta_2$ preincubated with indoline. Spectra were recorded 0.042, 0.0504, 0.0588, 0.0672, 0.0756, 0.1092, 0.126, 0.1596, 0.2436, 0.3276, 0.5376, 0.8736, 1.21, and 2.89 s following mixing. (C and D) Time courses at 466 nm for the reaction of L-Ser mixed in the SWSF apparatus with $\alpha_2\beta_2$, indoline, and different concentrations of CsCl (C) or NaCl (D). L-Ser (50 mM) and indoline (5 mM) were used for panels A–D, and the indicated MVC concentrations were used for panels C and D.

periods ranging from 3 to 80 min. At short incubation times, the traces show a strong dependence of the total amplitude on the incubation time; at longer incubation times, this dependence attenuates. For the sake of comparison, Figure 3B shows the SWSF time courses obtained for the indoline reaction when E(A-A) is premixed with various concentrations of NH_4^+ . The dependence of amplitude on NH_4^+ concentration increases and then becomes independent as the NH_4^+ concentration increases (Figure 3B).

Amplitudes measured at 466 nm provide a quantifiable measure of the fraction of E(Q)_{indoline} formed. Because of the magnitude of the fast phase, some amplitude is lost in the mixing dead time (viz., Figure 3A,B). To adjust for this loss, theoretical y-intercept values were calculated by extrapolation to the time of mixing. The NH_4^+ concentrations generated during each incubation period were estimated from the k_{cat} for pyruvate formation ($k_{\text{cat}} = 0.097 \text{ s}^{-1}$), the incubation time, and the concentration of enzyme. Corrected amplitudes then were plotted as a function of the NH_4^+ concentration [Figure 3C (●)]. For the sake of comparison, the amplitudes measured as a function of NH_4^+ concentration in Figure 3B were also plotted in Figure 3C (○). Figure 3C establishes that the amplitudes of the time courses taken from both panels A and B of Figure 3 depend upon the concentration of NH_4^+ . The apparent hyperbolic dependence of amplitude on NH_4^+ concentration indicates that these curves measure the apparent dissociation constant for NH_4^+ binding. When fitted to the positive lobe of a rectangular parabola, both data sets presented in Figure 3C yield a value of the apparent dissociation constant for NH_4^+ binding to the MVC site of ~0.67 mM.

Reaction of Preincubated MVC-Free $\alpha_2\beta_2$ and Indoline with L-Ser. To further investigate the reactivity of the MVC-free enzyme, MVC-free $\alpha_2\beta_2$ was preincubated with indoline and

Table 1: Effects of Saturating and Subsaturating Monovalent Cation Concentrations on the Indoline Reaction^a

| MVC | Wavelength of 466 nm | | | | | |
|--------------|----------------------|-----------------------------------|---------|-----------------------------------|---------|-----------------------------------|
| | A_1^b | $1/\tau_1\text{ (s}^{-1}\text{)}$ | A_2^b | $1/\tau_2\text{ (s}^{-1}\text{)}$ | A_3^c | $1/\tau_3\text{ (s}^{-1}\text{)}$ |
| MVC-free | 0.26 | 22.9 | 0.07 | 14.3 | 0.20 | 1.73 |
| CsCl, 0.5 mM | 0.66 | 40.3 | 0.39 | 9.2 | 0.13 | 1.20 |
| CsCl, 10 mM | 0.86 | 75.0 | 0.43 | 11.7 | 0.07 | 0.71 |
| NaCl, 0.5 mM | 1.38 | 10.7 | | | 0.50 | 1.98 |
| NaCl, 10 mM | 1.63 | 10.1 | | | 0.09 | 0.34 |
| MVC | Wavelength of 354 nm | | | | | |
| | A_1^b | $1/\tau_1\text{ (s}^{-1}\text{)}$ | A_2^b | $1/\tau_2\text{ (s}^{-1}\text{)}$ | A_3^b | $1/\tau_3\text{ (s}^{-1}\text{)}$ |
| MVC-free | 0.07 | 18.7 | | | 0.03 | 2.21 |
| CsCl, 0.5 mM | 0.07 | 34.7 | | | 0.02 | 1.83 |
| CsCl, 10 mM | 0.04 | 60.0 | | | 0.01 | 1.73 |
| NaCl, 0.5 mM | 0.04 | 13.7 | | | 0.05 | 1.63 |
| NaCl, 10 mM | 0.02 | 14.4 | | | 0.02 | 2.77 |

^aEnzyme and indoline in one syringe of the SWSF apparatus were mixed with indoline and L-Ser in the other syringe. The rates and amplitudes (absorbance changes) reported were derived from analysis of the time courses presented in Figure 4. ^bIncreasing absorbance. ^cDecreasing absorbance.

mixed with L-Ser in the SWSF apparatus (Figure 4A). The reaction was monitored at both 466 and 354 nm. At 466 nm, three relaxations were detected in the trace, two with increasing phases ($1/\tau_1 \approx 23\text{ s}^{-1}$, and $1/\tau_2 \approx 14\text{ s}^{-1}$) and one with a decreasing phase ($1/\tau_3 \approx 1.7\text{ s}^{-1}$) (Table 1). At 354 nm, two relaxation rates with increasing amplitudes were detected [$1/\tau_1 \approx 19\text{ s}^{-1}$, and $1/\tau_2 \approx 2.2\text{ s}^{-1}$ (Table 1)], values in good agreement with the rates of the first two relaxations observed at 466 nm for the formation of E(Q)_{indoline}.

RSSF time courses (Figure 4B) for the indoline reaction were measured to unambiguously identify the species formed during the three relaxations observed in Figure 4A. These time-resolved spectra establish that the absorbance changes at 466 nm accompanying $1/\tau_1$, $1/\tau_2$, and $1/\tau_3$ are due to the formation and decay of E(Q)_{indoline}. Figure 4B shows that after 0.16 s, the E(Q)_{indoline} band at 466 nm reaches an absorbance maximum and then decays, extrapolating to the absorbance values observed in MVC-free static spectra at the same enzyme concentration. Throughout the 2.89 s time interval for the RSSF experiment shown in Figure 4B, the band at 354 nm continues to increase in absorbance, and these changes are dominated by the formation of E(A-A). Kinetic slices from the RSSF data set measured at both 466 and 354 nm were fitted using PeakFit, and the relaxation rates were found to agree with those obtained from the SWSF time courses run under the same conditions (data not shown).

Panels C and D of Figure 4 compare the influence of Na⁺ and Cs⁺ on the SWSF time courses for the indoline reaction under conditions in which $\alpha_2\beta_2$ preincubated with indoline in one syringe was mixed with L-Ser preincubated with indoline in the other syringe. In panels C and D, the MVC was added to both syringes before the contents were mixed in the SWSF apparatus. In these 466 nm time courses, the decay of E(Q)_{indoline} observed at low Na⁺ or Cs⁺ concentrations either disappears or becomes obscured by the slow phases of increasing amplitude that appear as the MVC concentration increases. Table 1 summarizes rates and amplitudes measured at 466 and 354 nm for the MVC-free

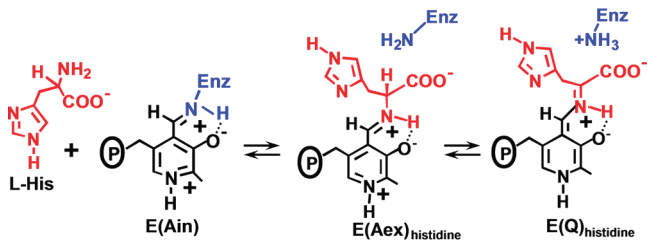
enzyme and compares these values with rates and amplitudes measured at subsaturating (0.5 mM) and saturating (10 mM) concentrations of Cs⁺ or Na⁺. The Cs⁺ form of the enzyme exhibited three phases at 466 nm (two increasing and one decreasing) and two phases at 354 nm (both increasing). The Na⁺ form of the enzyme exhibited two phases at 466 nm (one increasing and one decreasing) and two phases at 354 nm (both increasing).

Characterization of the MVC-Free E(A-A) Conformation. The data presented in Figures 2–4 establish that the reaction of MVC-free $\alpha_2\beta_2$ with L-Ser gives a MVC-free E(A-A) that is essentially inactive toward indoline. One possibility is that the inactive form of MVC-free E(A-A) has an open β -subunit conformation (9). In 1996, a method for probing the conformational state of tryptophan synthase, using the fluorescent ligand, 8-anilino-1-naphthalenesulfonate (ANS) was devised (35). When bound, ANS exhibits a strongly enhanced fluorescence emission spectrum; when free in aqueous solution, ANS exhibits a fluorescence that is strongly quenched. Pan and Dunn (35) demonstrated that ANS binds much more strongly to the open conformation than to the closed conformation of the tryptophan synthase $\alpha\beta$ -dimeric unit. Consequently, when the tryptophan synthase subunits switch to the closed conformation, ANS is released and fluorescence due to bound ANS is strongly decreased (35). To determine the conformational state of inactive MVC-free E(A-A), ANS fluorescence was used to probe the conformational states of the Na⁺, Cs⁺, and MVC-free forms of the enzyme. From the quenched ANS fluorescence, it was estimated that in the absence or presence of F9, L-Ser reaction displaces 81 or 89%, respectively, of bound ANS from the Cs⁺-bound enzyme, and 85 or 96%, respectively, of bound ANS from the MVC-free enzyme. These findings indicate that MVC-free E(A-A) adopts a closed conformation even though it is essentially inactive toward indoline.

Effects of F9 on the Formation and Decay of E(Q)_{indoline}. Ngo et al. (21, 22) demonstrated that the IGP analogue, F9, is a relatively specific, high-affinity ligand for the α -site and that F9 mimics the allosteric effects of product G3P. Like other IGP analogues, the binding of F9 stabilizes the closed conformation of the α -subunit, preventing the entry of indole and indole analogues such as indoline into the β -site from solution by blocking access to the interconnecting tunnel at the α -site (19, 21, 22, 33). Therefore, the use of F9 in combination with indoline provides a sensitive kinetic probe of the conformational switch to the closed conformation. When MVC-free $\alpha_2\beta_2$, preincubated with indoline, is mixed with L-Ser in the SWSF apparatus, there are two increasing phases ($1/\tau_1 \approx 20\text{ s}^{-1}$, and $1/\tau_2 \approx 10\text{ s}^{-1}$) and a decay phase ($1/\tau_3 \approx 2\text{ s}^{-1}$) (Figure 5, black trace). The time course also was examined under conditions in which the α -site is occupied by F9 (Figure 5, red trace). For this experiment, the F9 used was prepared free of monovalent metal ion. These data show that when F9 is bound to the α -site, the time course of the indoline reaction is changed; the F9 complex gives a slow increasing phase with a $1/\tau$ of $\sim 2\text{ s}^{-1}$, followed by a slow decreasing phase of very small amplitude with a rate that is reduced by a factor of 4 (Figure 5, red trace).

Influence of MVCs and F9 on the Reaction of L-His with E(Ain). L-His reacts with E(Ain) to form a distribution of covalent adducts at the β -active site dominated by the

corresponding external aldimine and quinonoid species (36) (eq 5).



UV-vis absorption spectra of the L-His reaction provide a means for quantifying the dependence of the distribution of E(Aex)_{histidine} and E(Q)_{histidine} species on the binding of MVCs and α-site ligands. Spectra were recorded with Cs⁺, NH₄⁺, Na⁺, and MVC-free forms of the enzyme, both in the absence (Figure 6A) and in the presence of F9 (Figure 6B). For the Cs⁺ and NH₄⁺ forms, these spectra exhibit contributions from two species, E(Aex)_{histidine} ($\lambda_{\text{max}} = 414 \text{ nm}$) and E(Q)_{histidine} ($\lambda_{\text{max}} = 470 \text{ nm}$) (37). The spectra of the MVC-free and Na⁺ forms are dominated by E(Aex)_{histidine} and show only trace amounts of E(Q)_{histidine} (~1.5 and ~2%, respectively). For each of the MVC-bound complexes, comparison of panels A and B of Figure 6 reveals a significant increase in the fraction of enzyme sites occupied by E(Q)_{histidine} when F9 is bound to the α-site (from ~2 to ~18.2% for Na⁺, from ~14 to 100% for NH₄⁺, and from ~17.3 to ~89% for Cs⁺). The percentages of E(Q)_{histidine} and E(Aex)_{histidine} formed were estimated from the static spectra and are summarized in Table 2. The simplifying assumption (eq 5) was made that the observed spectral bands in the static spectra arise from E(Aex)_{histidine} and E(Q)_{histidine} and that contributions from E(GD)_{histidine} or E(Ain) are minor and can be neglected (16).

The effects of Cs⁺ and Na⁺ on the formation of E(Q)_{histidine} when $\alpha_2\beta_2$ is titrated with L-His in the presence of F9 were determined. L-His has a slightly higher affinity for the Cs⁺ form of the enzyme than for the Na⁺ form, giving K_D values of 6 and 11 mM, respectively (data not shown). Binding of F9 increases the affinity of the Cs⁺ and Na⁺ forms of the enzyme for L-His ~3-fold. Figure 6C shows that the affinity of F9 for the L-His complex is enhanced ~10-fold by the substitution of Cs⁺ for Na⁺.

Analysis of the Effects of Cs⁺ Substitution for Na⁺ on Open and Closed Structures. The comparison of β-subunit structures was accomplished using alignment by sequence of the Cα atom positions for residue 10 to 100 with PyMOL. Comparison of indole subsites was accomplished using paired selections consisting of the MVC and atoms in the PLP cofactor.

The superposition of the Na⁺ and Cs⁺ forms of the β-subunit in the closed conformation shows very small structural differences. The most significant changes include the following. (a) Cs⁺ is displaced relative to the position of Na⁺ by ~1 Å. (b) Na⁺ is coordinated by the carbonyl oxygens of βGly232, βPhe306, and βSer308 and two waters, while Cs⁺ is coordinated by the carbonyl oxygens of βGly232, βPhe306, βSer308, βVal231, βGly268, and βLeu304 and one water molecule. (c) Those residues involved in coordination show a slight perturbation when Na⁺ is replaced with Cs⁺, with the largest effect on βGly232 (positional shift of ~0.4 Å). (d) In all of the β-subunit closed structures, the side chain of βAsp305 takes up a single orientation, a swing out position pointing away from the active site, and makes a salt bridge with βArg141. (e) The side chains of βTyr279 and βPhe280 take up positions against the tunnel wall

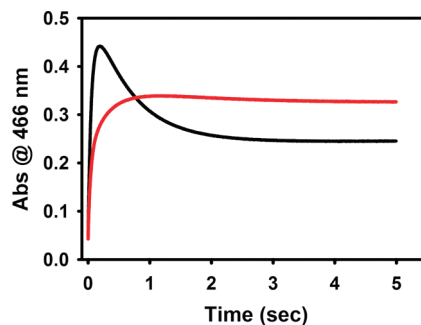


FIGURE 5: Comparison of time courses for the formation and decay of E(Q)_{indoline} in the presence and absence of the α-site ligand, F9. L-Ser and indoline in one syringe were mixed with $\alpha_2\beta_2$ and indoline in the other syringe of the SWSF apparatus in the presence (red) or absence (black) of F9. Final concentrations were 20 μM $\alpha_2\beta_2$, 50 mM L-Ser, 5 mM indoline, and 200 μM F9.

leaving the tunnel unhindered. In some structures, the side chain of βPhe280 is disordered.

In the open conformation, substitution of Cs⁺ for Na⁺ has a stronger effect on structure than in the closed conformation. Rhee et al. (6) made very careful comparisons of the effects of Na⁺, K⁺, and Cs⁺ on the structure of the open conformation. Their comparison of the Na⁺ and Cs⁺ complexes of E(Ain) used PDB entries 1BKS and 1TTP, respectively.² We re-examined the comparison of the Na⁺ and Cs⁺ forms of E(Ain) using a different structure for the Na⁺ complex, PDB entry 1KFK. We found that this Na⁺ structure differs significantly from PDB entry 1BKS only in the position of the βAsp305 side chain. The likely origins of this difference stem from the different temperatures used in the X-ray diffraction experiments (300 K for PDB entry 1BKS vs 100 K for PDB entry 1KFK). In PDB entry 1BKS, the side chain takes up two positions, a swing in position toward the active site and a swing out position pointed away. The more favored, swing-in, position makes a salt bridge with βLys167. In the structure of PDB entry 1KFK, the βAsp305 side chain takes up a somewhat different swing out position.

Kinetic Simulation of the Transient Formation and Decay of MVC-Free E(Q)_{indoline} in the Indoline Reaction. The formation of a closed, inactive E(A-A) species is consistent with Scheme 2 and is supported by the kinetic and spectroscopic results shown in Figures 4 and 5. Kinetic simulation was performed to further test the validity of Scheme 2 (for full details, see Figure S1 and Tables S1 and S2 of the Supporting Information). Because the binding of L-Ser and the conversion of E(Ain)(L-Ser) to E(Aex)₁ are relatively rapid processes, and because there is a strong forward commitment to give E(Aex)₁ (Scheme 2), these steps are decoupled from subsequent steps and do not perturb the rates of subsequent relaxations. Consequently for the simulations, Scheme 2 was simplified and rewritten as Scheme 3. Comparison of the simulated time courses with the experimental time courses obtained at both 466 and 350 nm shows good agreement (see Figure S1 of the Supporting Information). Furthermore, it was found that the effects of substitution of Cs⁺ for Na⁺ and the presence or absence of an MVC are well-accommodated by Scheme 3 (see Figure S1 and Tables S1 and S2 of the Supporting Information). For example, the experimental data and the corresponding simulations show that

²Although not stated by Rhee et al. (6), the Na⁺ structure used in the comparisons of conformation appears to be PDB entry 1BKS [a refined version of the original E(Ain) structure, PDB entry 1WSY].

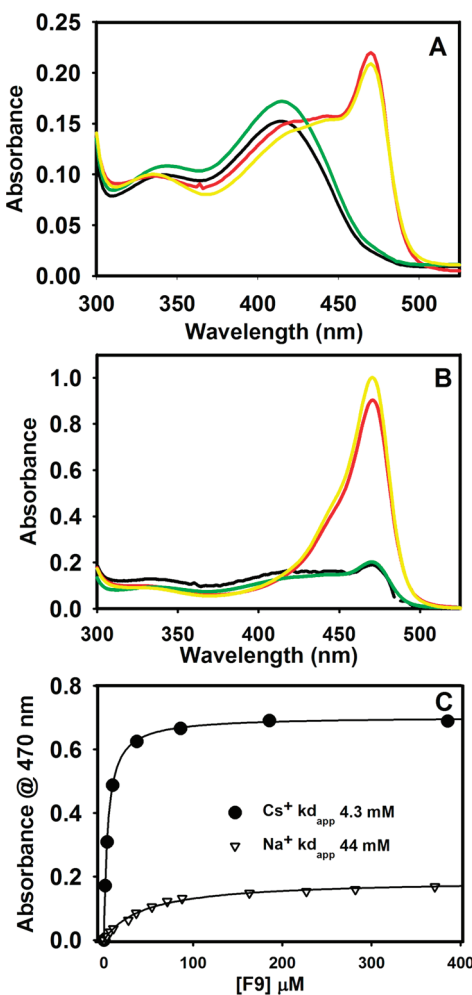


FIGURE 6: Static spectra for the reactions of various MVC forms of $\alpha_2\beta_2$ with l-His (eq 5) in the absence (A) and presence (B) of F9. MVC forms: Na⁺ (black), Cs⁺ (red), MVC-free (green), and NH₄⁺ (yellow). (C) Binding isotherms measured at 470 nm for the titration of F9 into a premixed solution of $\alpha_2\beta_2$, l-His, and Cs⁺ (●) or Na⁺ (▽). Each line is the least-squares best fit of the data. Final concentrations were 100 mM l-His, 50 mM MVC, 200 μ M F9 (when present), and 10 mM $\alpha_2\beta_2$ (A and C) or 20 μ M $\alpha_2\beta_2$ (B).

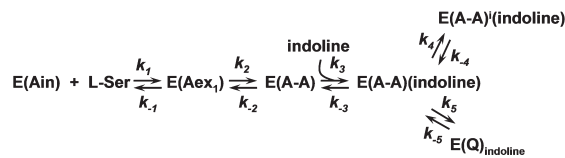
Table 2: Dependence of E(Q)_{his} Yield on the Binding of Monovalent Cations and on the α -Site Ligand, F9

| | estimated yield of E(Q) _{his} (%) ^a | |
|------------------------------|---|------------------|
| | without F9 | with F9 |
| MVC-free | ~1.5 | ~16.0 |
| Na ⁺ | ~2.0 | ~18.2 |
| NH ₄ ⁺ | ~14.0 | 100 ^b |
| Cs ⁺ | ~17.3 | ~89 |

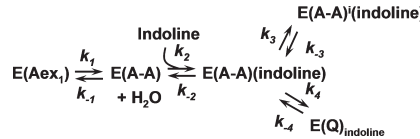
^aPercentages estimated from spectra in Figure 6. ^bThe yield obtained with the NH₄⁺ form of the F9 complex was assumed to be 100% of the β -sites.

when Cs⁺ is substituted for Na⁺, the fast relaxation is increased by >7-fold, whereas the MVC-free and Na⁺ forms of the enzyme show similar relaxation rates (22.9 and 10.1 s⁻¹, respectively) (see Table S2 of the Supporting Information). The >6-fold difference in amplitudes of the MVC-free and Na⁺ enzymes for this relaxation (0.26 Å vs 1.63 Å) are consistent with the conclusion that most of the MVC-free E(A-A) is present in an unreactive

Scheme 2: Formation of E(A-A) and Reaction with Indoline via the Branched Path for the Preincubation of E(Ain) with Indoline



Scheme 3: Simulation Scheme for Formation and Reaction of E(A-A) via the Simplified Branched Path



state while the reactive state predominates in the MVC-bound forms.

DISCUSSION

As is true for allosteric effectors in general, the action of MVCs in the regulation of enzyme activity and protein function has its origins in the modulation of protein conformation between states of altered activity. This modulation involves at least two levels of conformation hierarchy: global changes in subunit structure such as the switching between T and R states and local changes such as the perturbation of the dimensions and/or properties of a ligand binding site (25, 26). As discussed below, the results presented in this study demonstrate that the binding of an MVC is essential for switching between open (inactive) and closed (active) states of tryptophan synthase, and for maintenance of the correct conformation of the indole subsite at the β -subunit.

The influence of Na⁺ binding on the activation energies for steps in the β -reaction has been examined by Woehl and Dunn (10). They concluded that in stage I of the β -reaction Na⁺ binding (a) slightly stabilizes the binding of L-Ser to E(Ain), (b) strongly stabilizes E(Aex₁), (c) lowers the activation energy for E(Aex₁) formation, and (d) increases the activation energy for E(A-A) formation. In stage II, both the complex of indole with E(A-A) and E(Q) are stabilized by Na⁺ binding, while the activation energies for E(Q) formation and decay are unaffected by Na⁺ binding.

Analysis of Effects of MVCs on β -Subunit Structure and Function. The ionic radii of Na⁺, K⁺, and Cs⁺ are 0.97, 1.33, and 1.74 Å, respectively. This size variation dictates MVC-dependent differences in coordination number and geometry for inner sphere ligand complexes in small molecules and in proteins (25). The MVC effects described in this work and in previous studies no doubt have their origins in the propagation of these differences from the MVC site to the surrounding protein (6–10, 27). Alignment of β -subunit structures taken from the protein database shows only two global conformations of the β -subunit, the open conformation typically found for E(Ain) and E(Aex₁) and the closed conformation recently determined for an E(A-A) complex (21, 22) and for a quinonoid complex (20). Closed β -subunit structures have also been reported for two different tryptophan synthase mutants (38, 39). There are no published structures for MVC-free forms of the enzyme. Because the open conformation is easily crystallized, most structural studies have focused on the Na⁺ form of the

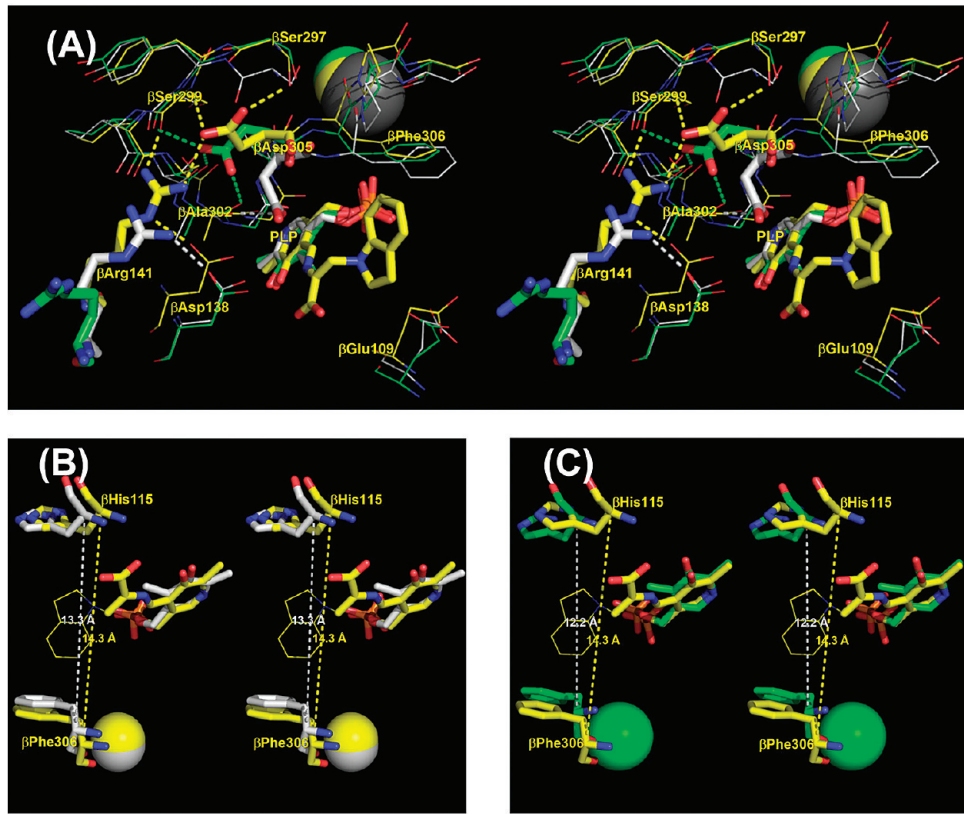


FIGURE 7: (A) Stereoscopic diagram comparing details of the β -sites and MVC sites of the Na^+ – and Cs^+ –E(Ain) complexes (PDB entries 1KFK and 1TTP, respectively) with the Cs^+ –E(Q)_{indoline} complex (PDB entry 3CEP). The E(Ain) complexes have the open β -subunit conformation, and the E(Q)_{indoline} complex has the closed conformation. Structures were aligned using the C α atom coordinates of β -subunit residues 10–100. For PDB entry 1KFK, carbons, Na^+ , and dashes are colored gray. For PDB entry 1TTP, carbons, Cs^+ , and dashes are colored green. For PDB entry 3CEP, carbons, Cs^+ , and dashes are colored yellow. All other atoms are shown in CPK colors. β Asp305, β Arg141, and the PLP moieties are shown as sticks, and other residues are shown as wireframe diagrams. Dashed lines indicate H-bonds and/or van der Waals contacts among the side chain of β Asp305, β Arg141, and nearby residues. (B and C) Stereoviews comparing the indole subsites of the open Cs^+ – and Na^+ –E(Ain) complexes, respectively, with the closed Cs^+ –E(Q)_{indoline} complex. In panels B and C, the C and Cs^+ atoms are colored yellow in the Cs^+ –E(Q)_{indoline} complex. In panel B, the C and Cs^+ atoms of the Cs^+ –E(Ain) complex are colored gray. In panel C, the C and Na^+ atoms of the Na^+ –E(Ain) complex are colored green. All other atoms are shown with CPK coloring. The indoline ring of the Cs^+ –E(Q)_{indoline} complex is shown as a wireframe diagram. The dashed lines measure the distances between the C α atoms of β His115 and β Phe306. In panels B and C, structures were superimposed using atoms of the PLP moieties and the MVC in the PyMOL-paired selection mode. Structures rendered with PyMOL version 1.1r1.

enzyme with the β -subunit in this conformation. However, there are six crystal structures of the enzyme with the β -subunit in the closed conformation, four of the Na^+ form [β -subunit mutants with β Lys87 replaced with Thr (PDB entries 2TRS, 2TRY, and 2TYS) and the mutant with β Gln114 replaced with Asn (PDB entry 2J9Y)] and two of the Cs^+ form [wild-type enzyme (PDB entries 3CEP and 2J9X)]. These structures make possible comparisons of the effects of substitution of Cs^+ for Na^+ on the closed conformation of the β -subunit.

Rhee et al. (6) described and compared the structures of the Na^+ , K^+ , and Cs^+ forms of E(Ain) in which the β -subunit has the open conformation. The salient findings of Rhee et al. (6) are summarized as follows. (a) When Cs^+ (PDB entry 1TTP) is substituted for Na^+ in E(Ain), significant changes are found in the locations of certain key β -site residues.² (b) Substitution of Cs^+ for Na^+ shifts Cs^+ ~1.1 Å from the Na^+ position. (c) Na^+ coordinates the carbonyl oxygens of β Gly232, β Phe306, and β Ser308 and two waters, while the Cs^+ coordination sphere expands to include β Val231, β Gly268, and β Leu304, but no waters. (d) The MVC binding loop (residues β 259– β 310) is slightly displaced by Cs^+ substitution, with the largest effects on β Phe306 and β Asp305 (positional shifts of ~0.8 Å). (e) In the

Na^+ structure, the β Tyr279 and β Phe280 side chains partially block the tunnel connecting the α - and β -sites. In the Cs^+ structure, these side chains take up positions against the tunnel wall and may cause a repositioning of α Asp56.

Figure 7A presents a composite overlay that compares details of the β -sites and MVC sites of the wild-type enzyme for the open β -subunits of the Na^+ (PDB entry 1KFK)^{2,3} and Cs^+ (PDB entry 1TTP) structures of E(Ain) with the closed β -subunit of the Cs^+ (PDB entry 3CEP) structure of E(Q)_{indoline}. The open structures of the Na^+ –E(Aex₁) complexes [PDB entries 1KFJ and 1KFE (40) and PDB entries 2CLL, 2CLM, and 2CLO (22)] all show placements of the β Asp305 side chain that are essentially identical to the position found in the Na^+ –E(Ain) complex (not shown). Figure 7A shows that the replacement of Na^+ with Cs^+

²The structure of PDB entry 1KFK used in place of PDB entry 1BK5 (Figure 7) differs only in the position of the β Asp305 side chain. The likely origins of this difference stem from the different temperatures used in the X-ray diffraction experiments (300 K for PDB entry 1BK5 vs 100 K for PDB entry 1KFK). In PDB entry 1BK5, the side chain takes up two positions, a swing-in position toward the active site and a swing-out position pointed away. The more favored, swing-in, position makes a salt bridge with β Lys167. In the structure of PDB entry 1KFK, the β Asp305 side chain takes up a somewhat different swing-out position with Oδ1 contacting the carbonyl O of β Ala302.

gives an open E(Ain) structure where the side chain of β Asp305 is shifted toward the position found in the closed Cs^+ conformation (the swing out position). Previous structural and kinetic studies (4, 5, 11, 20, 22, 34, 38, 39) strongly indicate that formation of the H-bonded salt bridge between β Asp305 and β Arg141 with the associated H-bonding network involving β Ser197 and β Ser199 (Figures 1B and 7A) is essential both for conversion of the β -subunit from the open to the closed conformation and for activation of the β -site for the conversion of E(Aex₁) to E(A-A) and E(Q) (Scheme 1). The K⁺-substituted E(Ain) complex (PDB entry 1TTQ) shows the side chain of β Asp305 in a position nearly identical to that found in the Cs⁺-E(Ain) complex, the swing out position (6). Thus, increasing MVC size favors the swing out position for the β Asp305 side chain, a conformation that is poised to form the salt bridge with β Arg141 when the β -subunit is switched to the closed conformation. Since the MVC site of tryptophan synthase *in vivo* likely is occupied by K⁺, these comparisons (Figure 7A) suggest that the Cs⁺ structures are better models for the physiologically relevant form of E(Ain) than are the Na⁺ structures. Accordingly, we hypothesize that the MVC effects reported in this work result from shifts between the open and closed states caused by the preferential stabilization of one state relative to the other by the particular MVC.

Detailed comparisons of the indole ring subsite (Figure 7B) show that the open Cs⁺-E(Ain) and closed Cs⁺-E(Q)_{indoline} complexes have very similar cavities for the indole ring (modeled by the indoline group), whereas the open Na⁺-E(Ain) complex exhibits a somewhat different cavity (Figure 7C). The rings of β Phe306 and β His115 define the long dimension of the indole subsite cavity (Figure 7B,C). Figure 7B shows that these residues are similarly aligned both in open and in closed Cs⁺ complexes, with the cavity diameter decreased by ~ 1.0 Å (measured as the distance between the β His115 and β Phe306 C α positions) in the open E(Ain) structure compared to the closed E(Q)_{indoline} structure. However, in the open Na⁺ complex, β His115 is shifted relative to the positions found in the Cs⁺ complexes and the diameter of the cavity is reduced by ~ 2 Å compared to that of the closed E(Q)_{indoline} structure (Figure 7C). Comparisons of the closed Cs⁺-E(Q)_{indoline} and Cs⁺-E(A-A) complexes and the closed Na⁺ complexes of E(Aex) species (38) show that all the indole cavities in these closed conformations are very similar even though the cavity is only partially filled in some of these structures (data not shown). These comparisons establish that the indole cavities of the open Na⁺-E(Ain) and Na⁺-E(Aex₁) complexes are collapsed and/or distorted relative to the cavities of the closed structures. As argued in the following paragraphs, this constriction or distortion of the cavity in the open conformation of the Na⁺-bound enzyme likely accounts for the MVC-dependent differences reported herein.

Effects of Ligand Binding on Stage I of the β -Reaction. Kinetic and spectroscopic studies in aqueous solution have established that ligand binding to three different loci, the α - and β -catalytic sites and the MVC site (Figure 1), can alter the distribution of covalent intermediates formed in stages I and II of the β -reaction (Scheme 1). It is now clear that these ligand-induced changes in distribution result from the switching of the β -subunit between the open and closed conformational states (5, 22).

Figure 2A compares the effects of MVCs on the interconversion of the open E(Aex₁) and closed E(A-A) complexes. As shown in Figure 2A, stage I of the β -reaction gives a distribution of intermediates that is MVC-dependent. This distribution is

determined by the relative stabilities of the MVC complexes of the open E(Aex₁) ($\lambda_{\max} = 424$ nm) and closed E(A-A) species ($\lambda_{\max} = 354$ nm, shoulder at 460 nm). The spectra show that for NH₄⁺ and Cs⁺, conversion to E(A-A) is nearly complete, indicating that both ions have a significantly higher affinity for E(A-A) than for E(Aex₁). For Na⁺ complexes, although E(A-A) is still the predominant species, there is a significant amount of E(Aex₁) present at equilibrium. The open Na⁺-E(Aex₁) complex [like the Na⁺-E(Ain) complex (21, 22)] has an active site with the side chains of β Asp305 and β Arg141 incorrectly positioned to form the salt bridge, and the indole subsite has a collapsed or distorted structure (viz. Figure 7). Since the open Cs⁺-E(Ain) complex and all known closed structures with either Na⁺ or Cs⁺ bound have preformed indole binding sites in the β -subunit (viz. Figure 7B), it is reasonable to conclude that the reason Na⁺ is less effective than NH₄⁺ and Cs⁺ in stabilizing E(A-A) is because the difference in Na⁺ affinity for E(Aex₁) versus E(A-A) is smaller.

Effects of Binding of MVC and ASL on the Reaction of L-His with E(Ain). L-His reacts with MVC-bound forms of tryptophan synthase to give equilibrating mixtures of E(Aex)_{his} and E(Q)_{his} (eq 5). Figure 6 and Table 2 show that the MVC-free and Na⁺ forms of the enzyme react with L-His to give E(Aex)_{his} with only small amounts of E(Q)_{his}, ~ 1.5 and $\sim 2\%$, respectively, whereas the Cs⁺ and NH₄⁺ forms give ~ 17.3 and $\sim 14\%$, respectively. Binding of the α -site ligand, F9, gives ~ 16 , ~ 18 , ~ 89 , and $\sim 100\%$ E(Q)_{his} for the MVC-free, Na⁺, Cs⁺, and NH₄⁺ enzymes, respectively. These findings establish that Na⁺ is ineffective in stabilizing E(Q)_{his}, whereas binding of NH₄⁺ and Cs⁺ causes a significant reordering of the relative stabilities of E(Aex)_{his} and E(Q)_{his} in favor of E(Q)_{his} (Figure 6A). The binding of ASLs further stabilizes the NH₄⁺ and Cs⁺ forms of E(Q)_{his} (Figure 6B) but exerts only a small effect on the Na⁺ forms. By analogy to the L-Ser and indoline reactions, it is likely that E(Aex)_{his} has the open conformation while E(Q)_{his} has the closed conformation. Binding of L-His to give E(Aex)_{his} is ineffective in displacing ANS, indicating the conformation of this species is open (35). Therefore, the stabilizing effects of NH₄⁺ and Cs⁺ on E(Q)_{his} likely reflect higher affinities of these MVCs for the closed conformation of E(Q)_{his} than for the open conformation of E(Aex)_{his}. Conversely, the difference in affinity of Na⁺ for E(Aex)_{his} and E(Q)_{his} must be relatively small. The further stabilization of E(Q)_{his} by the ASL, F9 (Figure 6B), is consistent with a ligand-induced allosteric shift in favor of the closed state (4, 5, 11, 22, 33, 36, 37, 41). The trend toward tighter binding at the β -site (Figure 6C) is similar to that seen with L-Ser; for example, F9 binds 25-fold more tightly to closed E(A-A) ($K_D \sim 2 \mu\text{M}$) than to open E(Ain) ($K_D \sim 50 \mu\text{M}$) (22).

All of the reported ligands specific for the α -site appear to exert allosteric interactions that favor the closed β -subunit conformation (5, 22, 42) (Figures 5 and 6). In stage I of the β -reaction, the binding of unreactive indole analogues (e.g., benzimidazole) to the β -subunit indole subsite shifts the distribution of species completely to E(A-A) in the closed β -subunit conformation (33, 36, 37). The substitution of NH₄⁺ or Cs⁺ for Na⁺ at the MVC site also shifts the distribution of species essentially completely to E(A-A) in the closed β -subunit conformation (4, 8–11, 20, 22) (Figure 2).

Reactivity of E(A-A) with Indoline. This work and previous studies show that indoline reacts rapidly and reversibly with MVC-bound forms of E(A-A) to give E(Q)_{indoline} (Figures 2–5) (8–10, 17–19, 33). At concentrations of indoline

approaching saturation of binding, there is little difference in yield for these MVC-bound forms. However, because the apparent dissociation constant for indoline is MVC-dependent, at 5 mM indoline the yields of E(Q)_{indoline} shown in Figure 2B are substantially different among the MVC-free and MVC-bound forms of the enzyme (8). Consequently, under the conditions described in the legend of Figure 2B, the Na⁺-bound enzyme is converted to E(Q)_{indoline} in nearly quantitative yield, while the Cs⁺-bound and NH₄⁺-bound enzymes give 60–70 and 30–40%, respectively. The experiments presented in Figures 3 and 4 establish that the amount of E(Q)_{indoline} formed (~3.5%) in the absence of added MVC is due either to contaminating MVC [likely NH₄⁺ generated by the pyruvate side reaction (eq 2)] or to a residual amount of active, MVC-free E(A-A).

When L-Ser is reacted with MVC-free $\alpha_2\beta_2$ preincubated with indoline, three relaxations are observed at 466 nm, two with increasing phases and one with a decreasing phase (Figure 4). Comparison of time courses shows, as expected, that E(A-A) formation and E(Q)_{indoline} formation are kinetically linked. These indoline reaction time courses indicate that the MVC-free enzyme reacts with L-Ser to give a mixture of active and inactive E(A-A) forms strongly weighted toward the inactive form (Figure 4). The time courses in Figure 4 show that when L-Ser reacts with the MVC-free enzyme in the presence of indoline, the reactive MVC-free E(A-A) initially formed is quickly consumed by reaction with indoline to give MVC-free E(Q)_{indoline}. In this experiment (Figure 4), the rate of formation of E(Q)_{indoline} is determined by the rate of formation of the active MVC-free E(A-A) from E(Aex₁) which is limited by the rate of E(A-A) formation, a process occurring at ~20 s⁻¹ (9). The slow decay (1/τ₃ ≈ 2 s⁻¹) at 466 nm and the slow increase (1/τ₂ ≈ 2 s⁻¹) at 354 nm reflect the conversion of active E(A-A) to inactive E(A-A) (9, 10), and the results presented here agree with this conclusion. Consequently, the slow decay of MVC-free E(Q)_{indoline} occurs in response to the slow redistribution of enzyme forms in favor of inactive E(A-A) (Figure 4). Thus, conversion to inactive E(A-A) occurs at the expense of E(Q)_{indoline}. The bifurcated pathway in Scheme 2 describes the partitioning of active E(A-A) between E(Q)_{indoline} and inactive E(A-A). Because formation of E(Q)_{indoline} is rapid and reversible, and conversion to inactive E(A-A) is slow, this scheme predicts that formation of E(Q)_{indoline} will show a transient increase and decrease, just as is seen in Figure 4. The relaxation for the slow interconversion (~2 s⁻¹) is present in the time courses both for the formation of E(A-A) and for the decay of E(Aex₁) (9). This slow process is most likely due to a conformational change that transforms active E(A-A) into the inactive species.

ANS has been shown to be a sensitive probe of tryptophan synthase conformational states (35, 42). ANS is displaced when the subunits are switched from the open to the closed conformations. ANS is displaced when E(A-A) is formed regardless of whether an MVC is bound. This finding is consistent with the assignment of closed conformations for both the active and inactive MVC-free E(A-A) species. Since the nucleophilic attack of indoline on E(A-A) is the step most effected in the indoline reaction by removal of the MVC, it seems likely that the switch from active to inactive MVC-free E(A-A) involves a structural rearrangement of the β-subunit indole binding subsite that interferes with the binding of indoline. The switch from the open to the closed conformation of the β-subunit as E(Aex₁) is converted to E(A-A) (Scheme 1) creates a relatively high-affinity binding site capable of binding indole and indole analogues such

as benzimidazole or indoline, and this conformation is stabilized by MVC binding. We propose that without a bound MVC, this subsite slowly relaxes to a “collapsed” conformation, effectively decreasing the affinity of indoline and interfering with formation of E(Q)_{indoline}. The binding of Na⁺ either prevents or makes negligible the conformational transition to the collapsed conformation, allowing accumulation of E(Q)_{indoline} in nearly stoichiometric amounts (Figures 2 and 3).

Effect of α-Site Ligand Binding on the Formation of Inactive E(A-A). In the absence of an ASL, reaction of indole or indole analogues with E(A-A) to give E(Q) is relatively rapid (200–900 s⁻¹, depending on the MVC and the substrate) (31, 33, 43–46). ASL binding to the α-site with the β-site in the form of E(A-A) switches both the α- and β-subunits to the closed conformation, thus greatly retarding the entry of ligands from solution into the sites and the interconnecting tunnel (5, 18, 19, 21, 22, 32, 33, 42, 47). Figure 5 shows the influence of the high-affinity α-site ligand, F9 (21, 22), on the formation and decay of E(Q)_{indoline} under MVC-free conditions. When L-Ser is mixed with F9-bound $\alpha_2\beta_2$ and indoline under MVC-free conditions, two increasing phases are seen at 466 nm with a 1/τ₁ of ≈20 s⁻¹ and a 1/τ₂ of ≈2 s⁻¹, followed by a decay phase very small in amplitude (Figure 5, red trace). The presence of F9 does not effect the rate of E(A-A) formation at 354 nm (data not shown), yet the decay phase at 466 nm (compare the black and red traces), observed in the absence of F9, disappears almost entirely. Therefore, it appears that the binding of F9 to the α-site shifts the equilibrium shown in Scheme 2 toward the active branch of the E(A-A) system, thus increasing the yield of E(Q)_{indoline} and reducing the fraction of sites in the inactive E(A-A) form. This result establishes that F9 binding to the α-site and MVC binding to the β-site have similar effects on the distribution of active and inactive forms of MVC-free E(A-A), and these effects are synergistic.

Kinetic Simulation of MVC-Free E(Q)_{indoline} Formation and Decay. Substitution of Cs⁺ for Na⁺ increases the rate of E(Q)_{indoline} formation by >7-fold, whereas the MVC-free and Na⁺ forms of the enzyme show similar relaxation rates (22.9 and 10.1 s⁻¹, respectively). In this latter comparison, it is important to notice that there is a strong influence of the MVC on reaction amplitude (>6-fold) (see Table S2 of the Supporting Information).

By adjusting the forward and reverse rates for the step responsible for the formation of inactive E(A-A) according to Scheme 3, we simulated the effects of Na⁺ and Cs⁺ binding on the formation and decay of E(Q)_{indoline}. Comparison of the experimental data with these simulations shows good agreement (see Figure S1 and Table S2 of the Supporting Information), confirming that the fast formation phase corresponds to the observed rate of formation of E(A-A) for the Na⁺, Cs⁺, and MVC-free forms of the enzyme (9). Therefore, these simulations support a model (Schemes 2 and 3) in which there are two possible fates for E(A-A): either the electrophilic β-carbon of E(A-A) reacts with indoline to form E(Q)_{indoline}, or E(A-A) remains in an inactive state with indoline noncovalently bound. It is our assessment that the two branches shown in Scheme 2 occur under any MVC condition; however, the inactive E(A-A) branch is of little significance when the MVC site is occupied.

In contrast to the effects caused by MVC substitutions, the absence of a bound MVC impairs the reactions of nucleophiles such as indoline and indole with the α-aminoacrylate intermediate (Figures 2–4) and significantly destabilizes quinonoid species

(Figure 6). Although reaction of L-Ser initially generates a reactive E(A-A), this species decays to an inactive state within a few seconds (Figures 3, 4, and 7). Reactivity is restored by the binding of MVCs and is partially preserved by the binding of ASLs (Figures 5 and 6). We conclude that the decay of the active MVC-free E(A-A) to an inactive state results from a conformational transition that compromises the structural integrity of the indole subsite of the β -subunit.

CONCLUSIONS

Metal ion-activated proteins are present throughout nature; however, the mechanisms of activation are very diverse (25, 26). In tryptophan synthase catalysis and regulation, cation activation is achieved through an allosteric linkage connecting the PLP active site to the MVC binding site, a distance of ~ 8 Å (Figures 1 and 7). The MVC site consists of backbone carbonyls from a stretch of amino acids that can twist and bend to coordinate cations of different sizes and incorporate ligated water molecules as needed to satisfy the electrostatic requirements of the bound MVC.

These studies establish that without a bound MVC, both the reaction of indoline with E(A-A) and the reaction of L-His with E(Ain) are strongly impaired. The reaction of L-Ser with MVC-free E(Ain) gives a reactive but relatively unstable E(A-A) species that converts to an inactive form. The binding of Na^+ , NH_4^+ , or Cs^+ repairs β -site reactivity in the indoline reaction (Figures 2–4 and Table 1) and restores allosteric communication (8–10). In the reaction of E(Ain) with L-His, the binding of NH_4^+ or Cs^+ restores activity to E(Ain), but the binding of Na^+ does not. The binding of a high-affinity ASL (Figures 4 and 6 and Table 2) also restores reactivity to the MVC-free β -site and acts synergistically with MVCs to stabilize E(A-A) and E(Q) species.

Consequently, MVC binding ensures the structural integrity needed by the β -active site during stage II of the β -reaction both for the nucleophilic attack of indole and indole analogues on E(A-A) and for the conversion of E(Q) to E(Aex), then to E(GD) and E(Ain), and finally to the new amino acid as the catalytic cycle is completed. The origins of the deleterious effects of removal of the MVC from the β -subunit are reasonably explained as being due to the collapse or distortion of the indole ring subsite within the closed conformation of the β -subunit. Determination of the structural details of the perturbed site must await further studies.

In the tryptophan synthase system, the efficient channeling of substrate indole between the α - and β -sites requires the switching of $\alpha\beta$ -dimeric units of the tetrameric enzyme between open (active) and closed (inactive) conformational states (5, 25, 33, 42). Under normal *in vivo* conditions, the bienzyme complex likely exists in an inactive (“resting”) state with the α - and β -subunits in open conformations with the α -site unoccupied and the β -site in the form of E(Aex₁). IGP binding switches the α -subunit to the closed conformation, triggering a switch in the β -subunit from the resting E(Aex₁) state to a reactive closed conformation that then undergoes reaction to give E(A-A). This conformational switch activates the cleavage of IGP to indole and G3P at the α -site. The closed conformation of the $\alpha\beta$ -dimeric unit confines indole to the indole subsites of the α - and β -subunits and the interconnecting tunnel, ensuring reaction between indole and E(A-A) (as per Scheme 1). When the indole quinonoid species is converted to E(Aex₂), the dimeric unit is switched back to the open conformation, releasing G3P from the α -site as L-Trp is

formed in stage II of the β -reaction (5). The results presented here further substantiate the idea that the roles of bound MVC include stabilization of the β -subunit indole binding subsite and maintenance of a balance between the relative energies of the open and closed conformations of the β -subunit during catalysis (22, 25). This balance ensures that synchronization of the α - and β -catalytic cycles is achieved via ligand-mediated conformational switching between open and closed states of low and high activity (5).

SUPPORTING INFORMATION AVAILABLE

Results of the detailed kinetic simulation study consisting of Figure S1, Table S1, and Table S2. This material is available free of charge via the Internet at <http://pubs.acs.org>.

REFERENCES

1. Yanofsky, C., and Crawford, I. P. (1972) Tryptophan synthase. In *The Enzymes* (Boyer, P. D., Ed.) 3rd ed., pp 1–31, Academic Press, New York.
2. Miles, E. W. (1979) Tryptophan synthase: Structure, function, and subunit interaction. *Adv. Enzymol. Relat. Areas Mol. Biol.* **49**, 127–186.
3. Miles, E. W. (1991) Structural basis for catalysis by tryptophan synthase. *Adv. Enzymol. Relat. Areas Mol. Biol.* **64**, 93–172.
4. Miles, E. W., Rhee, S., and Davies, D. R. (1999) The molecular basis of substrate channeling. *J. Biol. Chem.* **274**, 12193–12196.
5. Dunn, M. F., Niks, D., Ngo, H., Barends, T. R. M., and Schlichting, I. (2008) Tryptophan synthase: The workings of a channeling nanomachine. *Trends Biochem. Sci.* **33**, 254–264.
6. Rhee, S., Parris, K. D., Ahmed, S. A., Miles, E. W., and Davies, D. R. (1996) Exchange of K^+ or Cs^+ for Na^+ induces local and long-range changes in the three-dimensional structure of the tryptophan synthase $\alpha_2\beta_2$ complex. *Biochemistry* **35**, 4211–4221.
7. Peracchi, A., Mozzarelli, A., and Rossi, G. L. (1995) Monovalent cations affect dynamic and functional properties of the tryptophan synthase $\alpha_2\beta_2$ complex. *Biochemistry* **34**, 9459–9465.
8. Woehl, E. U., and Dunn, M. F. (1995) Monovalent metal ions play an essential role in catalysis and intersubunit communication in the tryptophan synthase bienzyme complex. *Biochemistry* **34**, 9466–9476.
9. Woehl, E., and Dunn, M. F. (1999) Mechanisms of monovalent cation action in enzyme catalysis: The first stage of the tryptophan synthase β -reaction. *Biochemistry* **38**, 7118–7130.
10. Woehl, E., and Dunn, M. F. (1999) Mechanisms of monovalent cation action in enzyme catalysis: The tryptophan synthase α -, β -, and $\alpha\beta$ -reactions. *Biochemistry* **38**, 7131–7141.
11. Fan, Y. X., McPhie, P., and Miles, E. W. (1999) Guanidine hydrochloride exerts dual effects on the tryptophan synthase $\alpha_2\beta_2$ complex as a cation activator and as a modulator of the active site conformation. *Biochemistry* **38**, 7881–7890.
12. Drewe, W. F., Jr., and Dunn, M. F. (1985) Detection and identification of intermediates in the reaction of L-serine with *Escherichia coli* tryptophan synthase via rapid-scanning ultraviolet-visible spectroscopy. *Biochemistry* **24**, 3977–3987.
13. Drewe, W. F., Jr., and Dunn, M. F. (1986) Characterization of the reaction of L-serine and indole with *Escherichia coli* tryptophan synthase via rapid-scanning ultraviolet-visible spectroscopy. *Biochemistry* **25**, 2494–2501.
14. Hur, O., Niks, D., Casino, P., and Dunn, M. F. (2002) Proton transfers in the β -reaction catalyzed by tryptophan synthase. *Biochemistry* **41**, 9991–10001.
15. Phillips, R. S., Miles, E. W., Holtermann, G., and Goody, R. S. (2005) Hydrostatic pressure affects the conformational equilibrium of *Salmonella typhimurium* tryptophan synthase. *Biochemistry* **44**, 7921–7928.
16. Osborne, A., Teng, Q., Miles, E. W., and Phillips, R. S. (2003) Detection of open and closed conformations of tryptophan synthase by ¹⁵N-heteronuclear single-quantum coherence nuclear magnetic resonance of bound 1-¹⁵N-L-tryptophan. *J. Biol. Chem.* **278**, 44083–44090.
17. Roy, M., Keblawi, S., and Dunn, M. F. (1988) Stereoelectronic control of bond formation in *Escherichia coli* tryptophan synthase: Substrate specificity and enzymatic synthesis of the novel amino acid dihydroisotryptophan. *Biochemistry* **27**, 6698–6704.

18. Harris, R. M., and Dunn, M. F. (2002) Intermediate trapping via a conformational switch in the Na^+ -activated tryptophan synthase bienzyme complex. *Biochemistry* **41**, 9982–9990.
19. Harris, R. M., Ngo, H., and Dunn, M. F. (2005) Synergistic effects on escape of a ligand from the closed tryptophan synthase bienzyme complex. *Biochemistry* **44**, 16886–16895.
20. Barends, T. R. M., Domratcheva, T., Kulik, V., Blumenstein, L., Niks, D., Dunn, M. F., and Schlichting, I. (2008) Structure and mechanistic implications of a tryptophan synthase quinonoid intermediate. *ChemBioChem* **9**, 261–266.
21. Ngo, H., Harris, R., Kimmich, N., Casino, P., Niks, D., Blumenstein, L., Barends, T. R., Kulik, V., Weyand, M., Schlichting, I., and Dunn, M. F. (2007) Synthesis and characterization of allosteric probes of substrate channeling in the tryptophan synthase bienzyme complex. *Biochemistry* **46**, 7713–7727.
22. Ngo, H., Kimmich, N., Harris, R., Niks, D., Blumenstein, L., Kulik, V., Barends, T. R., Schlichting, I., and Dunn, M. F. (2007) Allosteric regulation of substrate channeling in tryptophan synthase: Modulation of the L-serine reaction in stage I of the β -reaction by α -site ligands. *Biochemistry* **46**, 7740–7753.
23. Suelter, C. H. (1970) Enzymes activated by monovalent cations. *Science* **168**, 789–795.
24. Evans, H. J., and Sorger, G. J. (1966) Role of mineral elements with emphasis on the univalent cations. *Annu. Rev. Plant Physiol.* **17**, 47–76.
25. Woehl, E. U., and Dunn, M. F. (1995) The roles of Na^+ and K^+ in pyridoxal phosphate enzyme catalysis. *Coord. Chem. Rev.* **144**, 147–197.
26. Paige, M. J., and Di Cera, E. (2006) Role of Na^+ and K^+ in Enzyme Function. *Physiol. Rev.* **86**, 1049–1092.
27. Weber-Ban, E., Hur, O., Bagwell, C., Banik, U., Yang, L.-H., Miles, E. W., and Dunn, M. F. (2001) Investigation of allosteric linkages in the regulation of tryptophan synthase: The roles of salt bridges and monovalent cations probed by site-directed mutation, optical spectroscopy, and kinetics. *Biochemistry* **40**, 3497–3511.
28. Yang, L., Ahmed, S. A., and Miles, E. W. (1996) PCR mutagenesis and overexpression of tryptophan synthase from *Salmonella typhimurium*: On the roles of β_2 subunit Lys-382. *Protein Expression Purif.* **8**, 126–136.
29. Riddles, P. W., Blakeley, R. L., and Zerner, B. (1979) Ellman's reagent: 5,5'-Dithiobis(2-nitrobenzoic acid)—a reexamination. *Anal. Biochem.* **94**, 75–81.
30. Milescu, L. (1994) Kinetic, version 3.11, Informatics Laboratory, National Institute of Biotechnology, Bucharest, Romania.
31. Drewe, W. F., Jr., and Dunn, M. F. (1986) Characterization of the reaction of L-serine and indole with *Escherichia coli* tryptophan synthase via rapid-scanning ultraviolet-visible spectroscopy. *Biochemistry* **25**, 2494–2501.
32. Brzovic, P. S., Sawa, Y., Hyde, C. C., Miles, E. W., and Dunn, M. F. (1992) Evidence that mutations in a loop region of the α -subunit inhibit the transition from an open to a closed conformation in the tryptophan synthase bienzyme complex. *J. Biol. Chem.* **267**, 13028–13038.
33. Dunn, M. F., Aguilar, V., Brzovic, P., Drewe, W. F., Jr., Houben, K. F., Leja, C. A., and Roy, M. (1990) The tryptophan synthase bienzyme complex transfers indole between the α - and β -sites via a 25–30 Å long tunnel. *Biochemistry* **29**, 8598–8607.
34. Ferrari, D., Yang, L. H., Miles, E. W., and Dunn, M. F. (2001) $\beta\Delta 305A$ mutant of tryptophan synthase shows strongly perturbed allosteric regulation and substrate specificity. *Biochemistry* **40**, 7421–7432.
35. Pan, P., and Dunn, M. F. (1996) β -Site covalent reactions trigger transitions between open and closed conformations of the tryptophan synthase bienzyme complex. *Biochemistry* **35**, 5002–5013.
36. Houben, K. F., Kadima, W., Roy, M., and Dunn, M. F. (1989) L-Serine analogues form Schiff base and quinonoidal intermediates with *Escherichia coli* tryptophan synthase. *Biochemistry* **28**, 4140–4147.
37. Houben, K. F., and Dunn, M. F. (1990) Allosteric effects acting over a distance of 20–25 Å in the *Escherichia coli* tryptophan synthase bienzyme complex increase ligand affinity and cause redistribution of covalent intermediates. *Biochemistry* **29**, 2421–2429.
38. Rhee, S., Parris, K. D., Hyde, C. C., Ahmed, S. A., Miles, E. W., and Davies, D. R. (1997) Crystal structures of a mutant (βK87T) tryptophan synthase $\alpha_2\beta_2$ complex with ligands bound to the active sites of the α - and β -subunits reveal ligand-induced conformational changes. *Biochemistry* **36**, 7664–7680.
39. Blumenstein, L., Domratcheva, T., Niks, D., Ngo, H., Seidel, R., Dunn, M. F., and Schlichting, I. (2007) βQ114N and βT110V mutations reveal a critically important role of the substrate carboxylate site in the reaction specificity of tryptophan synthase. *Biochemistry* **46**, 14100–14116.
40. Kulik, V., Weyand, M., Seidel, R., Niks, D., Arac, D., Dunn, M. F., and Schlichting, I. (2002) On the role of αThr183 in the allosteric regulation and catalytic mechanism of tryptophan synthase. *J. Mol. Biol.* **324**, 677–690.
41. Ferrari, D., Niks, D., Yang, L.-H., Miles, E. W., and Dunn, M. F. (2003) Allosteric communication in the tryptophan synthase bienzyme complex: Roles of the β -subunit aspartate 305-arginine 141 salt bridge. *Biochemistry* **42**, 7807–7818.
42. Pan, P., Woehl, E., and Dunn, M. F. (1997) Protein architecture, dynamics and allostery in tryptophan synthase channeling. *Trends Biochem. Sci.* **22**, 22–27.
43. Faeder, E. J., and Hammes, G. G. (1971) Kinetic studies of tryptophan synthase. Interaction of L-serine, indole, and tryptophan with the native enzyme. *Biochemistry* **10**, 1041–1045.
44. York, S. (1972) Kinetic spectroscopic studies of substrate and subunit interactions of tryptophan synthase. *Biochemistry* **11**, 2733–2740.
45. Lane, A. N., and Kirschner, K. (1983) The catalytic mechanism of tryptophan synthase from *Escherichia coli*. Kinetics of the reaction of indole with the enzyme-L-serine complexes. *Eur. J. Biochem.* **129**, 571–582.
46. Lane, A. N., and Kirschner, K. (1983) The mechanism of binding of L-serine to tryptophan synthase from *Escherichia coli*. *Eur. J. Biochem.* **129**, 561–570.
47. Leja, C. A., Woehl, E. U., and Dunn, M. F. (1995) Allosteric linkages between β -site covalent transformations and α -site activation and deactivation in the tryptophan synthase bienzyme complex. *Biochemistry* **34**, 6552–6561.